Title

Reduction of peristalsis-related gastrointestinal streak artifacts with dual-energy CT: a patient and phantom study.

Journal

Abdominal radiology (New York), 41(8)

ISSN

2366-004X

Authors

Winklhofer, Sebastian
Lambert, Jack W
Wang, Zhen Jane
et al.

Publication Date

2016-08-01

DOI

10.1007/s00261-016-0702-2

Peer reviewed

HHS Public Access

Author manuscript

Abdom Radiol (NY). Author manuscript; available in PMC 2017 August 01.

Published in final edited form as:

Abdom Radiol (NY). 2016 August ; 41(8): 1456–1465. doi:10.1007/s00261-016-0702-2.

Reduction of peristalsis-related gastrointestinal streak artifacts with dual-energy CT: a patient and phantom study

Sebastian Winklhofer[1,2], **Jack W. Lambert**[1], **Zhen Jane Wang**[1], **Yuxin Sun**[1], **Robert G. Gould**[1], **Ronald J. Zagoria**[1], and **Benjamin M. Yeh**[1]

[1]Department of Radiology and Biomedical Imaging, University of California San Francisco, 505 Parnassus Ave, M-372, Box 0628, San Francisco, CA 94143-0628, USA [2]Institute of Diagnostic and Interventional Radiology, University Hospital Zurich, University of Zurich, Raemistrasse 100, 8032 Zurich, Switzerland

Abstract

Objective—The purpose of the study was to assess the ability of rapid-kV switching (rs) dual-energy computed tomography (DECT) to reduce peristalsis-related streak artifact.

Methods—rsDECT images of 100 consecutive patients (48 male, 52 female, mean age 57 years) were retrospectively evaluated in this institutional review board–approved study. Image reconstructions included virtual monochromatic 70 and 120 keV images, as well as iodine(-water) and water(-iodine) material decomposition images. We recorded the presence and severity of artifacts qualitatively (4-point scale) and quantitatively [iodine/water concentrations, Hounsfield units, gray scale values (GY)] and compared to corresponding unaffected reference tissue. Similar measures were obtained in DECT images of a peristalsis phantom. Wilcoxon signed-rank and paired t tests were used to compare results between different image reconstructions.

Results—Peristalsis-related streak artifacts were found in 49 (49%) of the DECT examinations. Artifacts were significantly more severe in 70, 120, and water(-iodine) images than in iodine(-water) images (qualitative readout $P < 0.001$, each). Quantitative measurements were significantly different between the artifact and the reference tissue in 70, 120 keV, and water(-iodine) images ($P < 0.001$ for both HU and GY for each image reconstruction), but not significantly different in iodine(-water) images (iodine concentrations $P = 0.088$ and GY $P = 0.111$). Similar results were seen in the peristalsis DECT phantom study.

Correspondence to: Benjamin M. Yeh; Ben.Yeh@ucsf.edu.

Compliance with ethical standards

Conflict of interest Sebastian Winklhofer received grants from the Swiss National Science Foundation. Jack Lambert declares that he has no conflict of interest. Zhen Jane Wang received grants from the National Institutes of Health and is a shareholder of Nextrast, Inc. Yuxin Sun declares that she has no conflict of interest. Robert Gould declares that he has no conflict of interest. Ronald Zagoria received book royalties from Elsevier. Benjamin M. Yeh received grants from the National Institutes of Health, General Electric Healthcare, General Electric Global Research Center, received book royalties from Oxford University Press, and is a shareholder of Nextrast, Inc.

Informed consent The requirement for informed consent was waived by our Institutional Review Board.

Research involving human rights All procedures performed in studies involving human participants were in accordance with the ethical standards of the institutional and/or national research committee and with the 1964 Helsinki declaration and its later amendments or comparable ethical standards. The requirement for informed consent was waived by our Institutional Review Board.

Conclusions—Peristalsis-related streak artifacts seen in 70, 120 keV, and water(-iodine) images are substantially reduced in iodine(-water) images at rsDECT.

Keywords

Dual-energy computed tomography; Iodine image; Artifact reduction; Bowel peristalsis; Image quality

Artifacts in computed tomography (CT) may degrade image quality and compromise diagnostic accuracy. The types of CT image artifacts are numerous. In addition to physics-based artifacts (e.g., beam hardening, photon starvation, and metal artifacts) and scanner-based artifacts (e.g., ring, helical, and cone beam artifacts), patient-based artifacts (e.g., patient motion) common affect diagnostic CT images [1].

Motion artifacts from overall movement of a patient's body (e.g., respiration, head movements in brain scans) may be reduced by careful patient instruction or by proper patient positioning. However, the patient cannot control involuntary motion of internal organs, such as cardiac motion and intestinal peristalsis.

Peristalsis-related streak artifact is known to occur with conventional CT due to motion of intralumenal gas during imaging [2, 3]. Technical developments such as short scan times [4, 5] and software corrections [1] have reduced the frequency and severity of peristalsis-related streak artifacts, but such phenomena remain common in conventional CT and frequently impede accurate diagnosis [6].

Recently, the use of dual-energy computed tomography (DECT) has become increasingly recognized for its ability to improve clinical diagnoses. By imaging at two different tube potentials, DECT enables material differentiation based on differences in CT attenuation of materials imaged at high vs. low kVp [7]. Certain artifacts, such as metal streak artifact, is more severe at low than at high kVp settings. DECT has shown clinical value for reducing metal streak artifacts by allowing the construction of virtual monochromatic (VMC) high keV images that minimize metal streak artifacts beyond is possible with conventional CT high kVp imaging [8, 9].

However, the value of DECT for the reduction of peristalsis-related streak artifacts that occurs in bowel remains uninvestigated. The aim of our study was to assess the value of rapid-kV switching (rs) Dual-Energy Computed Tomography to reduce peristalsis-related streak artifact in abdominal scans.

Materials and methods

This was a retrospective study approved by our Committee on Human Research and compliant with requirements of the Health Insurance Portability and Accountability Act. Our institutional review board waived the need for patient consent.

Study population

We retrospectively identified 100 consecutive venous phase abdominal rsDECT scans from unique patients (48 male, 52 female, mean age 57 ± 15 years, range 22–88 years) performed in our institution. No oral contrast media or antispasmodic medication was given. No fasting was required prior to CT scanning. There were no inclusion criteria. Exclusion criteria were metallic foreign materials in the abdomen or pelvis ($n = 8$) and prior oral contrast material remaining in the bowel ($n = 4$). The indications for CT scanning were possible or known malignancy ($n = 43$), abdominal pain ($n = 21$), sepsis ($n = 19$), and other ($n = 17$).

Peristalsis phantom

A CT phantom was constructed to simulate intestinal peristalsis (Fig. 1). The experimental setup consisted of an expandable 100 mL vinyl bag (representing bowel) filled with either saline and air or with oral contrast (iohexol diluted to 7 mg iodine/mL) and air, and which was fixed at the bottom of a polyethylene tube (diameter 11 cm). Ninety 0.25 inch diameter plastic rods were placed around the vinyl bag to simulate hypodense lesions, and the polyethylene tube was then filled with water. During DECT scanning, the vinyl bag was alternately filled and emptied via a connected infusion tube (200 cm length) by manual injection and aspiration using a 60 cc luer lock syringe. The repeated injection and aspiration of saline into the bag resulted in a smooth expansion (inflated diameter 4.5 cm) and contraction (uninflated diameter 3 cm) of the vinyl bag.

Imaging and postprocessing

Imaging of both the phantom and of the patients was performed with a rsDECT scanner (Discovery CT750 HD, GE Healthcare, Waukesha, WI, USA) in dual-energy (gemstone spectral imaging or GSI) mode.

For each patient, the gemstone imaging (GSI) preset was chosen to approximate the CTDIvol of a scan obtained with 1.25 mm slice thickness, noise index 31, pitch 1:1.375, and ASIR 40%. Tube voltage, fast kilovoltage switching between 80 and 140 kVp.

Imaging of the phantom was performed using the same imaging parameters, with the GSI preset chosen to deliver a CTDIvol of 9.05 mGy. When filled with water and air, and again when filled with oral contrast and air, the phantom was scanned twice during active injection and aspiration of the vinyl bag, and twice without injection or aspiration of the vinyl bag. This imaging was repeated on the phantom using single energy CT at 120 kVp with 175 mA to achieve a similar CTDIvol of 9.03 mGy.

Postprocessing was performed on an Advantage Windows Server (Version 2.02, GSI Viewer, GE Healthcare, Waukesha, WI, USA) to generate 70 keV VMC images (resembling conventional 120 kVp polychromatic MDCT images), 120 keV VMC images, and the material density water(-iodine) and iodine(-water) image pairs. Except for the 120 keV VMC images, all reconstructions are routinely performed at our institution and are part of the basic types of images generated in abdominal DECT imaging. The additional reconstruction of VMC images of 120 keV was performed to investigate into artifact

reduction with higher keV images, which has previously been shown to reduce metal artifacts [10, 11].

Qualitative image analysis

The qualitative and quantitative image analysis was performed on a standard workstation (GSI viewer, AW Server 2.02, GE Healthcare, Waukesha, WI, USA) by two independent radiologists (R1, [*SW*] and R2 [*BMY*]) with 6 and 4 years of experience in abdominal DECT who were blinded to image type and to the results from the readout of the other data sets. R 1 performed image analysis in all 100 cases. To investigate into the intra-reader and inter-reader agreement, image analysis was repeated by R2 in 33 of the 100 cases (33%).

First, all 100 70 keV VMC examinations (resembling standard 120 kVp scans) were screened for the presence or absence of peristalsis-related streak artifacts in the abdomen. The readers recorded the segment of the bowel from which the peristalsis-related streak artifact originated (duodenum, jejunum, ileum, or colon), the organ that the artifact most affected (e.g., in liver tissue, in mesenteric fat, in bowel wall), and the qualitative artifact severity. The qualitative artifact severity was recorded on a 4-point scale: 1 = absence of streak artifact—full visibility of all surrounding tissues; 2 = minor or minimal streak artifact —minimal reduction of visibility of surrounding soft tissue; 3 = some or moderate streak artifact—moderately reduced visibility of surrounding soft tissue 4 = marked streak artifact —no anatomical details visible in the surrounding tissue [12]. For the qualitative readout of the phantom study, the surrounding simulated lesions were assessed by the Likert-scale described for scoring the patient scans.

Second, the qualitative artifact severity was recorded for the corresponding locations in the 120 keV, water(-iodine), and iodine(-water) images in the same way, each with one week latency to avoid recall bias. To assess intra-reader agreement, the qualitative image analysis was repeated by R1 in 20 consecutive cases of the detected cases with peristalsis-related streak artifacts after a time interval of one week to minimize recall bias.

Quantitative image analysis

The same two readers performed quantitative assessment of peristalsis-related streak artifact by manually drawing a circular region of interest (ROI) at least 1 cm^2 in size in the most visibly bright area of streak artifact in the 70 keV axial images. The ROI placement was then automatically populated simultaneously on to all other open reconstructions (120 keV, water(-iodine) images, and iodine(-water) images) in identical anatomical locations and with identical ROI-size.

For reference calculations, a second ROI measurement was performed in similar neighboring tissue without any artifacts (e.g., healthy liver tissue or unaffected mesenteric fat) in all datasets. Care was taken to avoid areas of inhomogeneity (i.e., tissue borders, vessels) and to avoid influence due to partial volume effect. Comparisons of quantitative measurements were performed between the artifact measurements and the reference tissue in each data set.

Quantitative measurements in monoenergetic images (70 and 120 keV) are given in HU, whereas quantitative measurements in water(-iodine) and iodine(-water) images are given in concentrations of the assessed material with units in mg/cc and 100 μg/cc, respectively.

In addition, gray scale images from all four datasets were exported to the local picture archiving and communication system (PACS) (Agfa, Mortsel, Belgium) and the same ROI measurements were performed in all datasets to assess differences of artifact intensity in gray scale units (GY) independent from material concentrations in water(-iodine) and iodine(-water) images.

Statistical analysis

Statistical analysis was performed using commercially available software (IBM SPSS Statistics, Version 21.0.: IBM Corp. Armonk, NY, USA). Categorical variables were expressed as frequencies and percentages; continuous variables were expressed as mean ± standard deviation (range). Testing for normality was performed using the Shapiro–Wilk test.

The intra-reader and inter-reader agreement for qualitative and quantitative imaging parameters was calculated by using weighted Cohen's κ-coefficients and intra-class correlation coefficients (ICC) statistics. Kappa values of 0.41–0.60 were interpreted as moderate, 0.61–0.80 were interpreted as substantial, and 0.81–1.00 as excellent agreement according to criteria originally proposed by Landis and Koch [13]. ICC values of 0.61–0.80 were interpreted as substantial, and 0.81–1.00 as excellent agreement according to criteria proposed by Landis and Koch [13].

The Wilcoxon signed rank test was carried out for comparison of qualitative artifact scores between 70, 120 keV, water(-iodine), and iodine(-water) images.

Pairwise comparison of quantitative values (HU, concentrations, and GY values) between 70, 120 keV, water(-iodine), and iodine(-water) images was carried out using the paired t-test. A P value of <0.05 was used to denote statistical significance.

Results

Patient study

In 49 (49%) of the 100 cases, intraabdominal peristalsis-related streak artifacts were detected. Of the 49 peristalsis-related streak artifacts, 32 (65%) were quantitatively and qualitatively assessable, whereas in 17 (35%) cases artifacts were only qualitatively assessable (e.g., bowel wall without enough surrounding reference tissue for quantitative ROI measurements). The origin of streak artifact was the stomach in 29 cases (59%), small bowel in 10 cases (20%), duodenal in seven cases (14%), and colonic in two cases (4%).

The organ most affected by the peristalsis-related streak artifacts was liver in 28 cases (57%), the bowel distal to the stomach in 11 cases (22%), the mesenteric fat in 6 cases (12%), and the gastric wall or lumen in 4 cases (8%). Image examples of artifacts are given in Figures 2, 3, and 4.

Qualitative results

The intra-reader agreement for the 4-point Likert-scale rating of artifact severity was excellent ($k = 0.83$, $P < 0.001$).

The intra-reader agreement for the 4-point Likert-scale rating of artifact severity was substantial ($k = 0.68$, $P < 0.001$).

Table 1 shows the results of the qualitative image analysis. The qualitative artifact scores were significantly ($P < 0.001$, each) lower for the iodine(-water) images (median score 1, range 1–2) compared to 70, 120 keV, and water(-iodine) images (median score 3, range 2–4, each). No significant differences were found in the qualitative artifact scores between 70 keV and water(-iodine) images ($P = 0.157$), between 70 and 120 keV images ($P = 0.317$), and between water(-iodine) images and 120 keV images ($P = 0.564$).

Quantitative results

The inter-reader agreement for the quantitative artifact assessment was excellent (ICC = 0.961 for HU) and (ICC = 0.976 for GY values).

Pairwise comparison of quantitative ROI measurements was used to assess the relationship between the peristalsis-related streak artifact and the surrounding reference tissue. The measured iodine concentrations were not significantly different in the artifacts compared to the unaffected reference tissue (22.91 × 100 μg/cc ± 7.3 vs. 22.41 × 100 μg/cc ± 6.4, respectively, $P = 0.088$). In contrast to the iodine(-water) images, the mean ROI measurements of the 70, 120 keV, and water(-iodine) images were significantly different (higher) in the areas of artifacts compared to the measured reference tissue (132.5 HU ± 25.2 vs. 84.62 HU ± 18.5 for 70 keV images, respectively, $P < 0.001$; 93.40 HU ± 23.5 vs. 42.75 HU ± 16.5 for 120 keV images, respectively, $P < 0.001$; and 1077.41 mg/cc ± 21.0 vs. 1027.62 mg/cc ± 13.6 for water(-iodine), respectively, $P < 0.001$).

Similarly, pairwise comparison of quantitative GY measurements showed no significant differences ($P = 0.111$) in mean measured iodine concentrations between the artifact (mean 48.88) and the surrounding reference tissue (mean 48.84) in iodine(-water) images. In contrast to the iodine(-water) images, mean quantitative GY measurements of the 70, 120 keV, and water(-iodine) images were significantly different (higher) in the areas of artifacts compared to the measured reference tissue (for 70 keV, 185.97 vs. 152.16, respectively; for 120 keV images, 166.00 vs. 128.90, respectively; and for water(-iodine) images, 193.19 vs. 148.16, respectively; $P < 0.001$ for all pairwise comparisons).

Phantom study

A total of ten areas of peristalsis-related streak artifacts were identified in the phantom without simulated oral contrast imaged during active injection and aspiration of saline. No peristalsis-related streak artifacts were seen in the scans without active injection or aspiration of the phantom. Pairwise comparison of the qualitative artifact scores demonstrated significantly less artifact severity for the iodine(-water) images (median score 1) compared to 70, 120 keV images, and water(-iodine) images (median score 3, each, $P < 0.005$ for each pairwise comparison to iodine(-water) scores). No significant differences

were found between 70 and 120 keV images ($P = 0.317$), 70 keV and water(-iodine) images ($P = 0.317$), or 120 keV and water(-iodine) images ($P = 1$).

A total of 11 areas of peristalsis-related streak artifacts were identified in the phantom with simulated oral contrast imaged during active injection and aspiration of saline. Again, no peristalsis-related streak artifacts were seen in the scans without active injection or aspiration of the phantom. Pairwise comparison of the qualitative artifact scores demonstrated significantly less artifact severity for the iodine(-water) images (median score 1) compared to 70, 120 keV images, and water(-iodine) images (median score 3, each, $P < 0.005$ for each pairwise comparison to iodine(-water) scores). No significant differenceswere found between 70 and 120 keV images ($P = 0.317$), 70 keV and water(-iodine) images ($P = 0.317$), or 120 keV and water(-iodine) images ($P = 0.157$).

Pairwise comparisons of quantitative GY ROI measurements in scans without simulated oral contrast showed no significant differences between the iodine(-water) mean artifact and the surrounding reference tissue values (16.0 vs. 15.4.3, respectively, $P = 0.217$). In contrast to the iodine(-water) images, mean quantitative GY measurements of the 70, 120 keV, and water(-iodine) images were significantly different (higher) in the areas of artifacts compared to the measured reference tissue (each $P < 0.001$; 160.8. vs. 101; 156.6 vs. 99.5; and 199 vs. 123.5, respectively, $P < 0.001$ for each pairwise comparison between areas of artifact and reference tissue).

Pairwise comparisons of quantitative GY ROI measurements in scans with simulated oral contrast showed significant differences for each pairwise comparison between areas of artifact and reference tissue in all datasets (each $P < 0.001$; 70 keV: 167.2. vs. 101.2; 120 keV 158.7 vs. 104.6; iodine(-water): 25.8 vs. 16.4.and water(-iodine) 194 .6 vs. 127.1).

Discussion

The results of our study show that rsDECT iodine(-water) images reduce peristalsis-related streak artifacts in abdominal scans. Iodine(-water) images effectively minimize or eliminate streak artifacts caused by intestinal peristalsis and improve the evaluation of adjacent tissues, such as the liver. Both qualitative and quantitative measurements revealed significantly less frequent and less severe artifacts in the iodine(-water) images as compared to the more conventional rsDECT 70 keV images, 120 keV monoenergetic images and water(-iodine) material density images. Our phantom study readily reproduced the peristalsis-related streak artifacts and supported the clinical scan findings that iodine(-water) images reduce peristalsis-related streak artifacts and improve the visibility of surrounding structures.

Our findings build on prior work showing that DECT can provide substantial benefits over that of single energy CT scanning. Prior work demonstrated that DECT can improve the evaluation of soft tissues around dense metal [14], improve the visualization and characterization of hyper- and hypovascular masses [15, 16], and differentiate density related to contrast material enhancement vs. underlying non-iodine radiodense material [17, 18]. Our findings show that rsDECT may provide particular benefit for patients where concerns relate to organs immediately adjacent to bowel.

We believe the suppression of peristalsis-related streak artifacts in the iodine images is a result of these artifacts behaving as a highly-attenuating version of water. In other words, their appearance is of a highly-attenuating material, causing the hyperdense streaking, however this attenuation remains relatively unchanged between the 80 and 140 kVp images, similar to water. Single-source rsDECT obtains projection data by the rapid alternation (within about 0.5 msec) between high (140 kVp) and low (80 kVp) tube potentials. Artifacts from streak appear to affect the high and low kVp data to a similar degree because they were assigned by the two material decomposition into the water(-iodine) image. As a result, these artifacts are correspondingly subtracted from the iodine image, thus revealing underlying tissue detail. This explanation is supported by the absence of any reduction in peristalsis-related streak artifact between the high monochromatic keV level images (120 keV) compared to the standard 70 keV images.

Peristalsis-related streak artifacts on internal organs during CT image acquisition may decrease image quality and may lead to erroneous diagnoses [19]. Since the peristaltic artifacts occur in the tissues immediately around the moving structures, the most affected organs are those immediately adjacent to bowel, such as liver, bowel, and mesentery. Although most diagnoses cannot be made with the iodine images alone, they can be used in combination with the other series available from the rsDECT scans to help enhance the image clarity and reveal otherwise obscured details.

Other published techniques for reduction of peristalsis-related streak artifacts can be patient-based, such as fasting prior to the examination or administration of antispasmodics (e.g., anticholinergic medications [20]), or technical–based, such as scan time reduction or software based correction algorithms [21–23]. Our finding that iodine(-water) images may be of value to further reduce artifacts and can be easily implemented in the daily clinical workflow. Future studies should be performed to assess whether DECT platforms other than rsDECT (e.g., dual-source or layer detector) could be used to obtain similar image reconstructions that reduce peristalsis-related streak artifacts.

Several limitations of this study deserve comment. First, our exploratory study did not investigate the clinical benefit of reduction of peristalsis-related streak artifacts. However, the general concern for bowel peristaltic artifacts is well known [24, 25]. Prospective studies are warranted to assess the value of this technique in clinical practice. Second, since the image appearances of the image reconstructions are very characteristic, no effective blinding to the type of image reconstruction was possible. However, the marked reduction in artifact at iodine(-water) images is fairly obvious, in retrospect. Thirdly, we only assessed 70 and 120 keV VMC images and we did not investigate higher keV data sets than 120 keV which may reduce certain types of artifact such as metal spray artifact. However, the artifacts persisted across the range that we studied, and from our experience with rsDECT, there is not as substantial a difference in image appearance between small changes in keV settings at higher X-ray energy. Future studies can explore whether VMC images can be further manipulated to improve peristalsis-related artifact.

In conclusion, rsDECT with iodine(-water) images enables significant reduction of peristalsis-related streak artifacts in abdominal imaging. Use of iodine(-water) images may assist in the evaluation of tissues adjacent to bowel.

Acknowledgement

This publication was supported by grants from the National Institutes of Health Grant Numbers 1R41DK104580 and 1R01EB015476, and the Swiss National Science Foundation grant P2SKP3_151973. Its contents are solely the responsibility of the authors and do not necessarily represent the official views of the National Institutes of Health or the Swiss National Science Foundation.

References

1. Barrett JF, Keat N. Artifacts in CT: recognition and avoidance. Radiographics. 2004; 24(6):1679–1691. [PubMed: 15537976]
2. Liu F, Cuevas C, Moss AA, et al. Gas bubble motion artifact in MDCT. AJR Am J Roentgenol. 2008; 190:294–299. [PubMed: 18212212]
3. Boas RE. CT artifacts: causes and reduction techniques. Imaging Med. 2012; 4:229–240.
4. Fleischmann D, Boas FE. Computed tomography–old ideas and new technology. Eur Radiol. 2011; 21(3):510–517. [PubMed: 21249371]
5. Rit S, Wolthaus JW, van Herk M, Sonke JJ. On-the-fly motion-compensated cone-beam CT using an a priori model of the respiratory motion. Med Phys. 2009; 36(6):2283–2296. [PubMed: 19610317]
6. Hamm, B.; Forstner, R.; Beinder, E. MRI and CT of the female pelvis. Springer; Berlin: 2007. p. 388
7. Silva AC, Morse BG, Hara AK, et al. Dual-energy (spectral) CT: applications in abdominal imaging. Radiographics. 2011; 31(4):1031–1046. discussion 47–50. [PubMed: 21768237]
8. Lee YH, Park KK, Song H-T, Kim S, Suh J-S. Metal artefact reduction in gemstone spectral imaging dual-energy CT with and without metal artefact reduction software. Eur Radiol. 2012; 22:1331–1340. [PubMed: 22307814]
9. Brook OR, Gourtsoyianni S, Brook A, et al. Spectral CT with metal artifacts reduction software for improvement of tumor visibility in the vicinity of gold fiducial markers. Radiology. 2012; 263:696–705. [PubMed: 22416251]
10. Bamberg F, Dierks A, Nikolaou K, et al. Metal artifact reduction by dual energy computed tomography using monoenergetic extrapolation. Eur Radiol. 2011; 21(7):1424–1429. [PubMed: 21249370]
11. Winklhofer S, Benninger E, Spross C, et al. CT metal artefact reduction for internal fixation of the proximal humerus: value of mono-energetic extrapolation from dual-energy and iterative reconstructions. Clin Radiol. 2014; 69(5):e199–e206. [PubMed: 24582174]
12. Lane BF, Vandermeer FQ, Oz RC, et al. Comparison of sagittal T2-weighted BLADE and fast spin-echo MRI of the female pelvis for motion artifact and lesion detection. AJR Am J Roentgenol. 2011; 197(2):W307–W313. [PubMed: 21785057]
13. Landis JR, Koch GG. The measurement of observer agreement for categorical data. Biometrics. 1977; 33(1):159–174. [PubMed: 843571]
14. Morsbach F, Bickelhaupt S, Wanner GA, et al. Reduction of metal artifacts from hip prostheses on CT images of the pelvis: value of iterative reconstructions. Radiology. 2013; 268(1):237–244. [PubMed: 23513244]
15. Yamada Y, Jinzaki M, Tanami Y, Abe T, Kuribayashi S. Virtual monochromatic spectral imaging for the evaluation of hypovascular hepatic metastases: the optimal monochromatic level with fast kilovoltage switching dual-energy computed tomography. Invest Radiol. 2012; 47(5):292–298. [PubMed: 22472797]
16. Kim KS, Lee JM, Kim SH, et al. Image fusion in dual energy computed tomography for detection of hypervascular liver hepatocellular carcinoma: phantom and preliminary studies. Invest Radiol. 2010; 45(3):149–157. [PubMed: 20142749]

17. Brown CL, Hartman RP, Dzyubak OP, et al. Dual-energy CT iodine overlay technique for characterization of renal masses as cyst or solid: a phantom feasibility study. Eur Radiol. 2009; 19(5):1289–1295. [PubMed: 19153744]
18. Stolzmann P, Frauenfelder T, Pfammatter T, et al. Endoleaks after endovascular abdominal aortic aneurysm repair: detection with dual-energy dual-source CT. Radiology. 2008; 249(2):682–691. [PubMed: 18780822]
19. Marmulla R, Muhling J. The influence of computed tomography motion artifacts on computer-assisted surgery. J Oral Maxillofac Surg. 2006; 64(3):466–470. [PubMed: 16487810]
20. Zand KR, Reinhold C, Haider MA, et al. Artifacts and pitfalls in MR imaging of the pelvis. Journal of magnetic resonance imaging : JMRI. 2007; 26(3):480–497. [PubMed: 17623875]
21. Zerfowski, D. Motion artifact compensation in CT.. Medical Imaging; Proceedings SPIE 3338; San Diego. 1998.
22. Yu H, Wang G. Data consistency based rigid motion artifact reduction in fan-beam CT. IEEE Trans Med Imaging. 2007; 26(2):249–260. [PubMed: 17304738]
23. Dhanantwari AC, Stergiopoulos S, Iakovidis I. Correcting organ motion artifacts in x-ray CT medical imaging systems by adaptive processing. I. Theory. Med Phys. 2001; 28(8):1562–1576. [PubMed: 11548927]
24. Kozak RI, Bennett JD, Brown TC, Lee TY. Reduction of bowel motion artifact during digital subtraction angiography: a comparison of hyoscine butylbromide and glucagon. Can Assoc Radiol J. 1994; 45(3):209–211. [PubMed: 8193968]
25. Rogalla P, Lembcke A, Ruckert JC, et al. Spasmolysis at CT colonography: butyl scopolamine versus glucagon. Radiology. 2005; 236(1):184–188. [PubMed: 15987972]

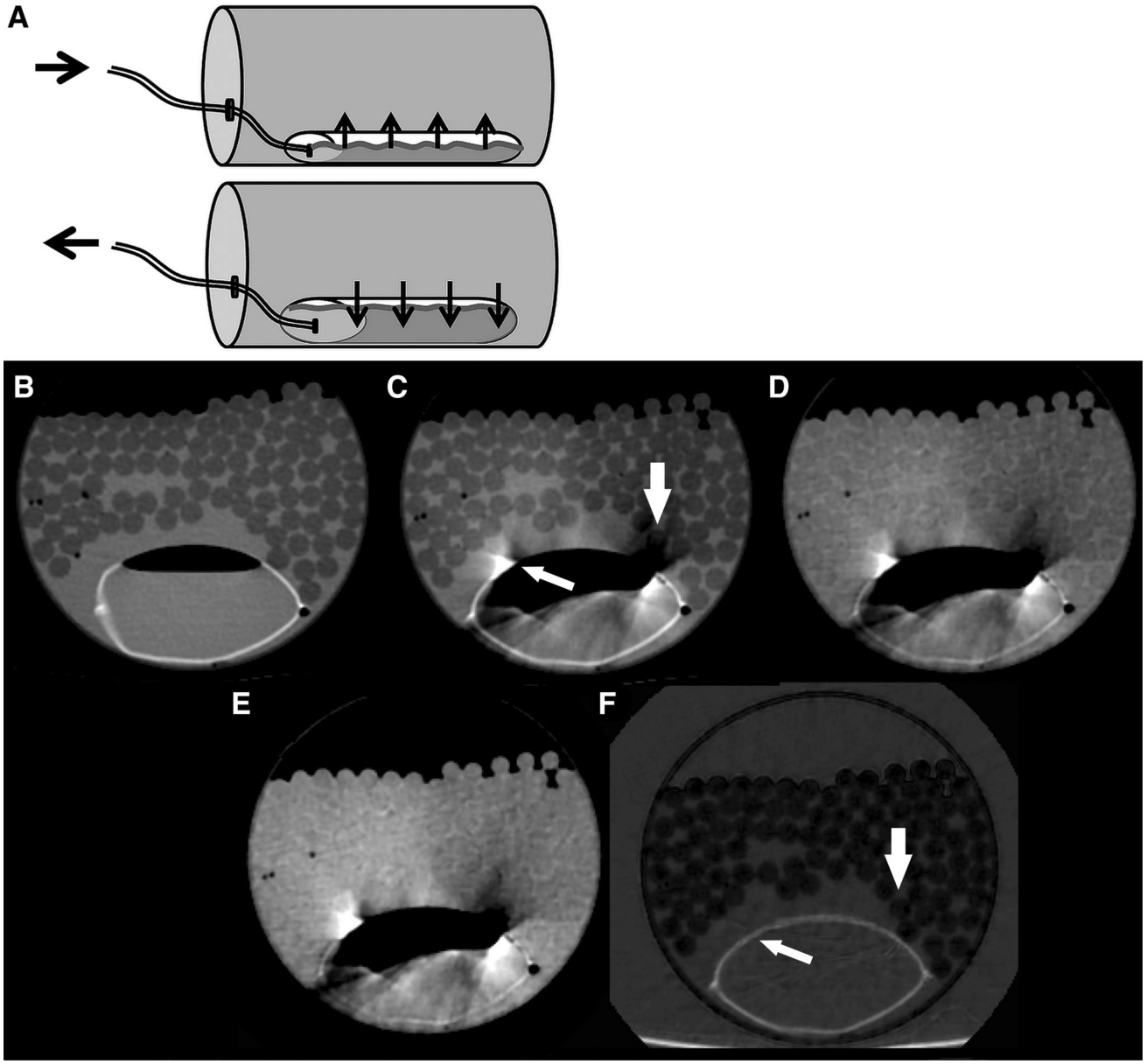

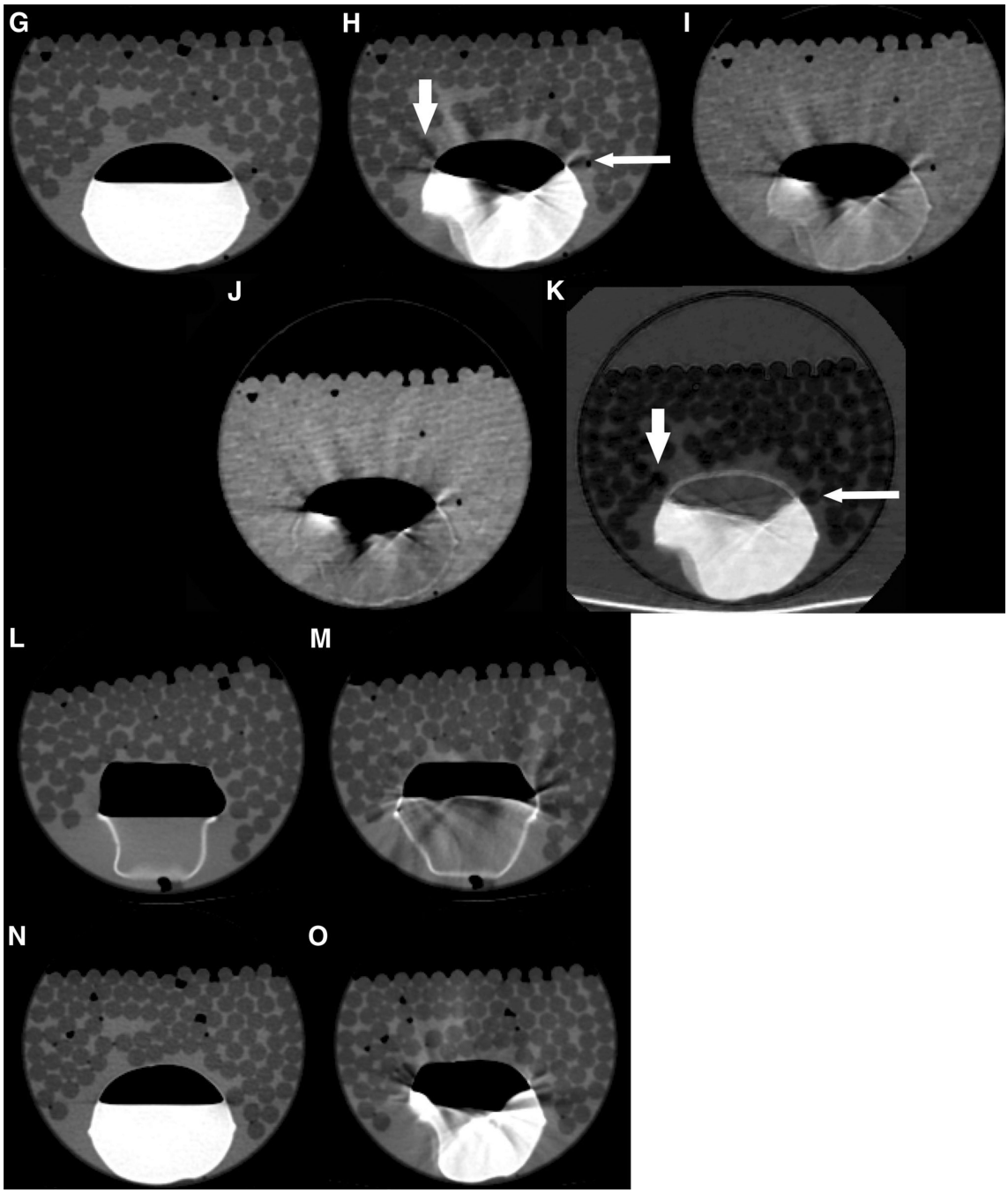

Fig. 1.

A Diagram of peristalsis CT phantom. A vinyl bag, simulating bowel, was fixed at the bottom of a rigid polyethylene tube filled with hypodense plastic rods and water. Images without dynamic injection at 70 keV, **B** without and **G** with oral contrast, did not show motion artifact. **C** and **H** 70 keV, **D** and **I** 120 keV, **E** and **J** water(-iodine) images, **F** and **K** iodine(-water) images CT images of the peristalsis phantom during simulated bowel peristalsis by injection and withdrawal of water and oral contrast into the vinyl bag, respectively. Note the reduced streak artifact in the iodine(-water) images compared to the

70, 120 keV, and water(-iodine) images, with less obscuration of surrounding water and simulated hypodense lesions (arrows). Single energy CT images with intraluminal water and oral contrast show motion artifact only with peristalsis (**M** and **O**) but not at rest (**N** and **L**).

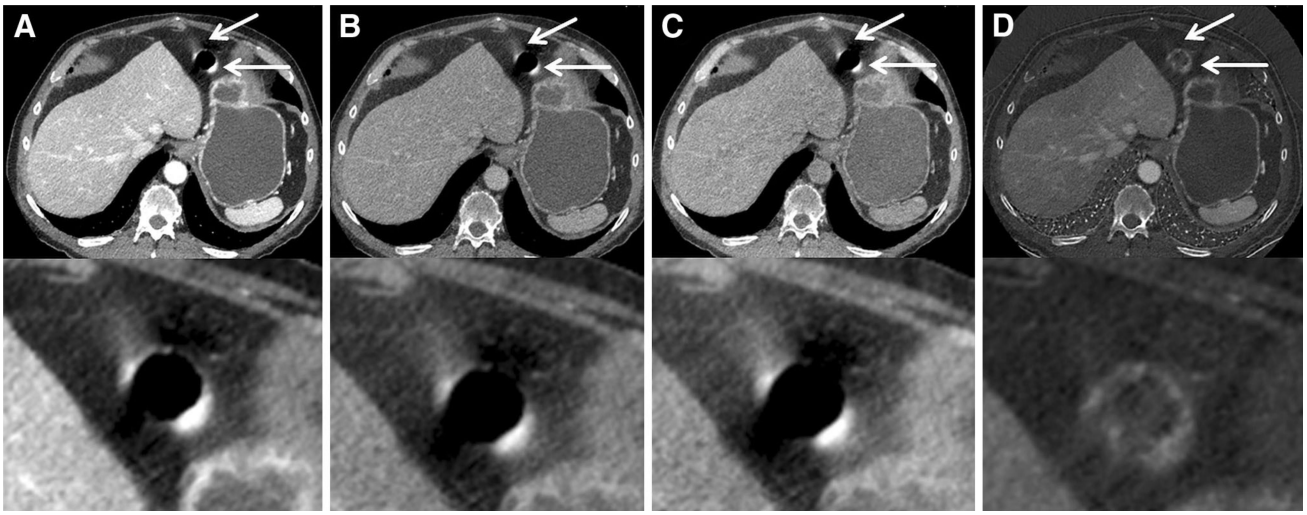

Fig. 2.

Axial Dual-Energy CT examination of the abdomen of a 59-year-old patient with corresponding magnified images. Peristalsis-related streak artifacts originate from the duodenum and most affect the intraabdominal fat (*arrows*). Note similar amounts of hyperdense streak artifacts in the (**A**) 70 keV, (**B**) 120 keV, and (**C**) water(-iodine) images. The artifacts are remarkably reduced in the iodine(-water) image (**D**).

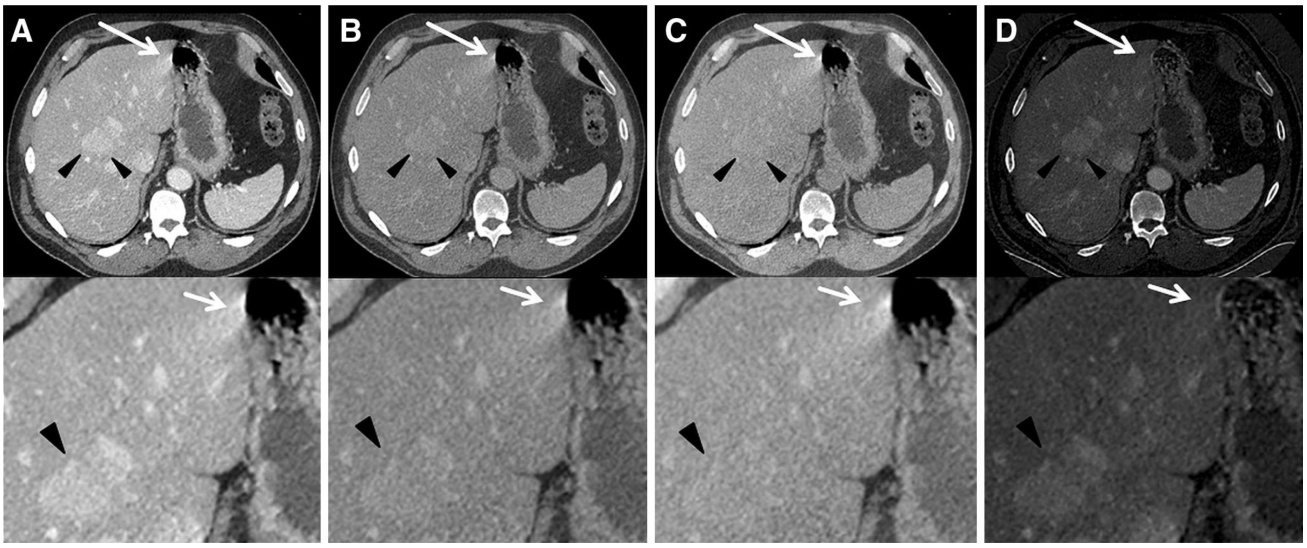

Fig. 3.

Axial Dual-Energy CT examination of the abdomen of a 57-year-old patient with known penile cancer. Gastric peristalsis-related streak artifact affects the liver the most (*arrows*). Corresponding magnified images are seen below each large field-of-view image. Prominent peristalsis-related streak artifact is seen in **A** 70 keV, **B** 120 keV, and **C** water (-iodine) images. Minimal peristalsis-related streak artifact is seen in the iodine(-water) image, **D** resulting in an improved visibility of the underlying liver tissue. *Note* Contrast enhancing hyperattenuating liver metastases with similar attenuation as the streak artifacts were seen (*arrowheads*) in this fatty liver.

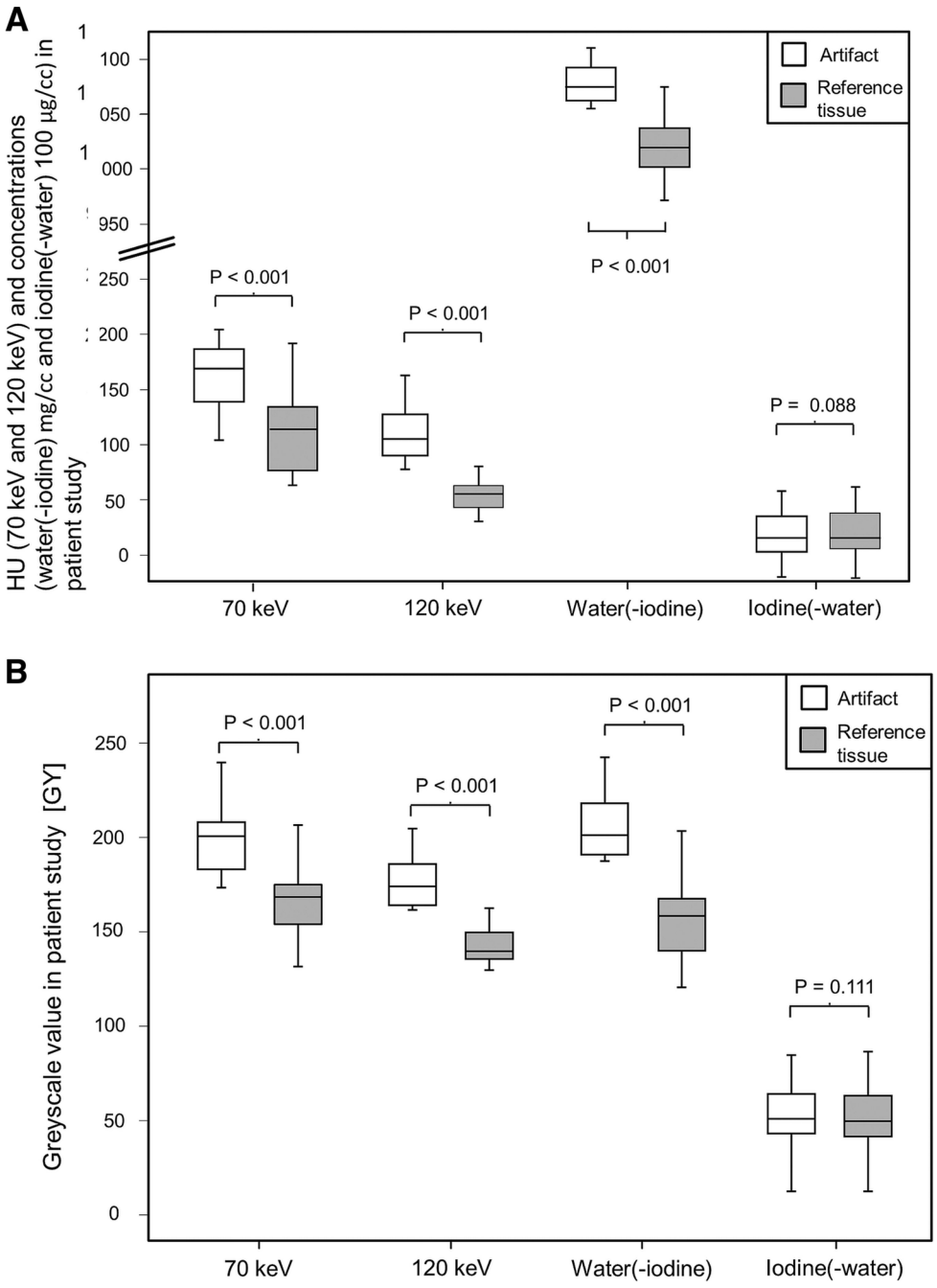

Fig. 4.

Box plots for quantitative assessment of ROI measurements of tissue affected and not affected by peristalsis-related streak artifacts. For 70 keV (resembling standard 120 kvP scan), 120 keV, and water(-iodine) images, significant differences between the artifact and the corresponding reference tissue were seen. No significant differences were seen for iodine(-water) images between tissue affected and not affected by peristalsis-related streak artifacts. **A** patient study; quantitative measurements in HU (70 and 120 keV) and

concentrations (water(-iodine) and iodine(-water) images). **B** patient study; quantitative measurements in *gray scale* units (GY).

Table 1

Image quality scores (4-point Likert scale) for the patient and phantom study of peristalsis-related streak artifacts in 70, 120 keV, water(-iodine), and iodine(-water) images

	Image quality (score)	70 keV	120 keV	Water(-iodine)	Iodine(-water)
Patients (artifacts $n = 49$)	1	0 (0%)	0 (0%)	0 (0%)	39 (80%)
	2	20 (41%)	19 (39%)	18 (37%)	10 (20%)
	3	22 (45%)	23 (47%)	24 (49%)	0 (0%)
	4	7 (14%)	7 (14%)	7 (14%)	0 (0%)
Phantom without oral contrast (artifacts $n = 10$)	1	0 (0%)	0 (0%)	0 (0%)	10 (100%)
	2	1 (10%)	0 (0%)	0 (0%)	0 (0%)
	3	5 (50%)	6 (60%)	6 (60%)	0 (0%)
	4	34 (40%)	4 (4%)	4 (40%)	0 (0%)
Phantom with oral contrast (artifacts $n = 11$)	1	0 (0%)	0 (0%)	0 (0%)	11 (100%)
	2	1 (9%)	1 (9%)	(0%)	0 (0%)
	3	5 (45.5%)	6 (54.5%)	6 (54.5%)	0 (0%)
	4	5 (45.5%)	4 (36.4%)	5 (45.5%)	0 (0%)

No peristalsis-related streak artifacts were seen in the phantom when it was imaged without active injection or aspiration of the simulated bowel